

Learning Privacy Preserving Encodings through Adversarial Training

Francesco Pittaluga¹ Sanjeev J. Koppal¹ Ayan Chakrabarti²

Abstract

We present a framework to learn privacy-preserving encodings of images (or other high-dimensional data) to inhibit inference of a chosen private attribute. Rather than encoding a fixed dataset or inhibiting a fixed estimator, we aim to learn an encoding function such that even after this function is fixed, an estimator with knowledge of the encoding is unable to learn to accurately predict the private attribute, when generalizing beyond a training set. We formulate this as adversarial optimization of an encoding function against a classifier for the private attribute, with both modeled as deep neural networks. We describe an optimization approach which successfully yields an encoder that permanently limits inference of the private attribute, while preserving either a generic notion of information, or the estimation of a different, desired, attribute. We experimentally validate the efficacy of our approach on private tasks of real-world complexity, by learning to prevent detection of scene classes from the Places-365 dataset.

1. Introduction

Images, videos, and other forms of high-dimensional data are rich in information about the environments they represent. This information can then be used to infer various environment attributes such as location, shapes and labels of objects, identities of individuals, classes of activities and actions, etc. But often, it is desirable to share data—with other individuals, with un-trusted applications, over an unsecured network, etc.—without revealing values of certain attributes that a user may wish kept private. For such cases, we seek an encoding or transformation of this data that is *privacy-*

preserving, in that the encoded data prevents or inhibits the estimation of specific sensitive attributes, but still retains other information about the environment—information that may be useful for inference of other, desirable, attributes.

When the relationship between data and attributes can be explicitly modeled, it possible to derive an explicit form for this encoding (Dwork, 2008). This includes the case where the goal is to encode a fixed dataset with known values of the private label (where privacy can be achieved, for example, by partitioning the dataset into subsets with different values of the private label, and explicitly transforming each set to the same value (Sweeney, 2002)). But in this work, we consider the case where the relationship between data and private attributes is not explicit, but instead is learned through training an estimation function.

We seek to find an encoding that prevents or inhibits such a trained estimator or classifier from succeeding. Note that we do not want an encoding that simply confounds a fixed classifier (or inference algorithm). Rather, we want that *even after the encoding is fixed*, a classifier that has knowledge of the encoding, and which can therefore be trained on encoded training data, is unable to make accurate predictions when generalizing beyond the training set. This is especially challenging because high-dimensional signals like images can contain multiple, redundant cues towards any environment attribute. While specific transformations can cause failures in given estimators that do not expect them, these estimators invariably recover when such transformations are included during training (Vasiljevic et al., 2016).

To address this issue, we present a formulation for *learning* an encoding function through adversarial training against a classifier that is simultaneously learning to succeed at inferring the private attribute on encoded data. The encoder, in turn, trains to prevent this inference, while also maintaining some notion of utility—a generic objective of maintaining variance in its outputs and optionally promoting the success of a second classifier training for a different attribute. We use deep neural networks to model both the classifier, as well as the encoder, and carry out optimization using gradient-based updates.

A key contribution of our work is in developing an approach for stable optimization of this complex min-max objective, which yields encoding functions that *permanently* limit re-

¹Department of Electrical and Computer Engineering, University of Florida, Florida, USA ²Department of Computer Science and Engineering, Washington University in St. Louis, Missouri, USA. Correspondence to: <f.pittaluga@ufl.edu>.

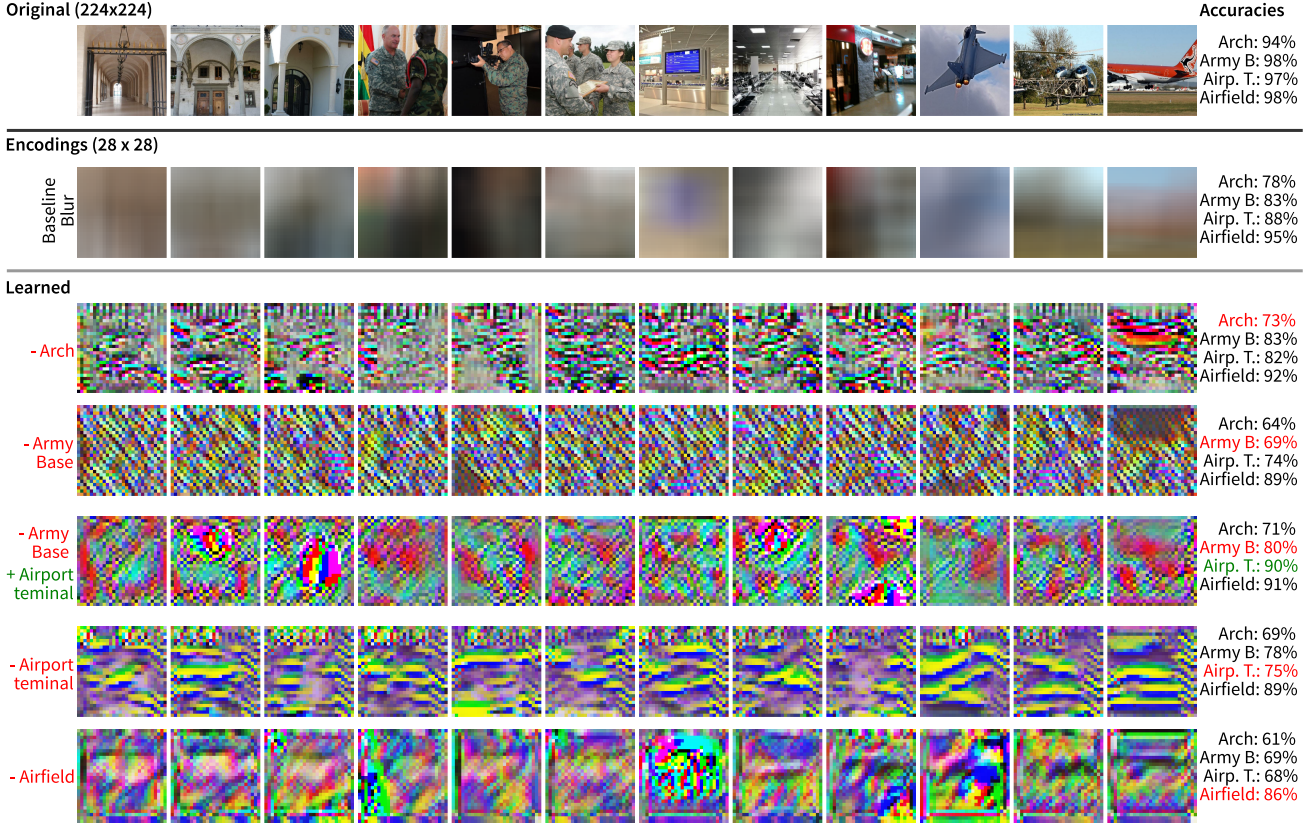


Figure 1. Privacy-preserving Encodings for Inhibiting Scene Class Detection. In each row we show positive example images from four different categories from the Places-365 dataset, arch, army-base, airport and air-field. In the far-right column we show the test accuracy for the four tasks when they are cast in a binary scene classification setting. The top row shows the original images and in the second row we show the output when a box filter of the same size as our encoder’s receptive field is applied on the original images. We use these blurred images as a baseline for privacy preservation. The last five rows show visualizations of the output of an encoder trained with our optimization, with the goal of inhibiting a negative task. For arch, army-base, airport terminal and airfield, we optimize using a generic objective maintaining variance in the encoder output. For army-base/airport terminal (center row), in addition to the generic objective, we optimize to promote a desired task. Red text indicates the negative task we are trying to inhibit and green text indicates a positive task we are trying to promote. Note that for the negative tasks (red text) we beat the blurring baseline. When we promote a desired task (green text) we also do better on it, in addition to inhibiting the negative task (red text).

covery of private attributes, while also maintaining some notion of utility. We demonstrate the efficacy of the approach through validation on tasks with real-world complexity. As illustrated in Fig. 1, our approach is able to successfully learn encoders that inhibit detection of different scene categories from encoded scenes from the Places-365 dataset (Zhou et al., 2017).

2. Related Work

There exist elegant approaches to privacy that provide formal guarantees (Dwork, 2008) when the relationship between data elements and sensitive attributes can be precisely characterized. This is true also for the special case when the privacy preserving task is aimed at a fixed dataset—in

which case the relationship is simply the enumerated list of samples and their attribute values, and approaches such as K-anonymity (Sweeney, 2002) can be employed. Our focus in this paper, however, is on applications where this relationship is not precisely known, and data elements to be censored are high-dimensional and contain multiple, redundant cues towards the private label that a learned estimator could be trained to exploit.

A lot of prior work on achieving privacy on achieving privacy with such data, especially with images and videos, has relied on domain knowledge and hand-crafted approaches—such as pixelation, blurring, face/object replacement, etc.—to degrade sensitive information (Boyle et al., 2000; Gross et al., 2008; Driessen & Durmuth, 2013; Agrawal & Narayanan, 2011; Yu et al., 2008; Chen et al., 2006). While

these methods are effective in many practical settings, they assume that a specific estimator, algorithm, or approach will be used to infer the private attribute, and seek to degrade the corresponding cues. In contrast, we assume that an adversary seeking to recover the private attribute will learn an estimator specifically for our encoding, and seek to limit its success. This makes the goal of learning an encoding significantly more challenging, since modern classifiers, such as those based on deep neural networks, are able to learn to make accurate predictions even from severely degraded data (e.g., see Vasiljevic et al. (2016)). It is also worth noting here recent works on finding adversarial examples (Goodfellow et al., 2014b; Nguyen et al., 2015; Moosavi-Dezfooli et al., 2016; Moosavi-Dezfooli et al., 2017). These methods learn perturbations (including “universal” perturbations (Moosavi-Dezfooli et al., 2017)) to cause incorrect predictions, but these are also trained against fixed classifiers.

This motivates our framework for *training* an encoding function, adversarially against a classifier being simultaneously trained to predict the private attribute. Our approach is motivated by the recent success of adversarial training for learning generative adversarial networks (GANs) (Goodfellow et al., 2014a), which demonstrated the feasibility of using stochastic gradient descent (SGD) to optimize a min-max objective involving deep neural networks with competing goals. Nevertheless, this optimization process is known to be very unstable (Arjovsky & Bottou, 2016). Moreover, our goal is to reach a point where the encoding function maintains its success even after it is fixed while its adversary continues to train. While such a stationary point exists theoretically given enough expressive power in the two competing networks (Goodfellow et al., 2014a), it is rarely achieved (or sought) in practice when training GANs. A key contribution of our work is in developing a stable optimization approach that has a lasting effect on classification ability for private attributes.

The closest formulations to ours are those of (Edwards & Storkey, 2015) and (Raval et al., 2017). These techniques also use adversarial optimization to learn image transformations that will prevent a classifier (trained on transformed images) from solving some sensitive task, along with the objective of the transformed image being as close to the original as possible (in terms of the squared difference of intensities). While these methods provide an interesting proof of concept, they target relatively simple private tasks—namely preventing the detection of synthetically superimposed text (Edwards & Storkey, 2015) or QR codes (Raval et al., 2017), and show that adversarial training learns to detect and blur the relevant regions. In contrast, we present an optimization approach that is demonstrated to work when training against classifiers for complex real-world tasks—namely scene recognition—on natural images. In particular, we show that our learned encoders succeed even where com-

parable blur baselines are unable to prevent detection of these global scene category labels.

3. Learning Private Encoding Functions

In this section, we describe our overall formulation and introduce our framework for learning privacy-preserving encoding functions with respect to specific sensitive tasks. We consider the following setting: when training the encoder, we have a training set labeled with values of the private attribute. Once the encoder has been trained, we seek to limit the ability of an adversary, with knowledge of this encoding function, to train an estimator for the private attribute.

In particular, we assume that after the encoder is fixed, the adversary will be able to train an estimator on an *encoded* labeled training set (by applying the encoding function on a regular training set), and we seek to restrict the performance of this estimator beyond that training set. We will measure this performance on encoded validation and test sets. Note that we do not seek to prevent the estimator from performing well on the training set itself, e.g., through memorization. Our goal is to limit generalization accuracy.

3.1. Privacy as Adversarial Objective

Formally, we seek an encoding function $E : \mathbb{R}^N \rightarrow \mathbb{R}^{N'}$ that maps a high-dimensional input (such as an image) $x \in \mathbb{R}^N$ to an encoded value $x' = E(x) \in \mathbb{R}^{N'}$, with the goal of preventing the estimation of a private attribute $u(x) \in \mathbb{U}$ from the encoded image x' . Consider a parameterized estimator $\Phi(x'; \theta_u)$ with learnable parameters θ_u that produces an estimate \hat{u} of $u(x)$ from the encoded image x' . Then, for some loss function $L(\hat{u}, u) : \mathbb{U} \times \mathbb{U} \rightarrow \mathbb{R}$, we define our desired encoding function as

$$E = \arg \max_E I(E; u), \quad (1)$$

where,

$$I(E; u) = \min_{\theta_u} \mathbb{E}_{p(x)} L(\Phi(E(x); \theta_u), u(x)). \quad (2)$$

Here, $I(E; u)$ can be thought of as the expected average loss of the best possible classifier Φ against a given encoder E . Note that this is a min-max optimization between the encoder E and classifier parameters θ_u .

There is clearly a trivial solution to the optimization of (2), namely where the encoder $E(x) = C$ outputs a constant value independent of the input. To avoid this, we impose a constraint on the statistics of the encoded outputs. Specifically, we require that on average (over samples of data x), each element of the encoded output have zero mean and unit variance, i.e., $\mathbb{E}E(x)_i = 0$ and $\mathbb{E}E(x)_i^2 = 1, \forall i \in \{1 \dots N'\}$, where $E(x)_i$ denotes the

i^{th} element of $x' = E(x)$. Therefore, the encoder is constrained to produce outputs with reasonable diversity, even as it tries to remove information regarding the label u . This constraint is aimed at maintaining information content in the encoded outputs, so that these outputs may be informative for estimating attributes other than u .

While a majority of our experiments will use only this generic constraint, our framework also allows an optimizing for utility with respect to one or more specific *desirable* attributes. Specifically, for such an attribute $v(x)$, we can define a corresponding $I(E; v)$ similar to (2):

$$I(E; v) = \min_{\theta_v} \mathbb{E}_{p(x)} L(\Phi(E(x); \theta_v), v(x)), \quad (3)$$

where the expectation can potentially be under a different distribution $p(x)$ for the desirable task. Then, we seek an encoder that trades off the goal of preserving v and inhibiting u with a scalar weight $\alpha > 0$ as:

$$E = \arg \max I_u(E) - \alpha I_v(E). \quad (4)$$

We enforce the zero mean and unit variance constraints on the encoder outputs for this case as well. Note that the objective above involves an adversarial optimization with a *collaboration* between the encoder E and desirable attribute classifier parameters θ_v , against the classifier parameters θ_u for the private attribute.

3.2. Architecture and Optimization

We use deep-neural networks to model the estimators $\Phi(\cdot; \theta_u)$ and $\Phi(\cdot; \theta_v)$. In particular, we consider binary attributes and Φ corresponds to a classifier trained with a log-loss L . We also use a deep neural network to model the encoder E , and the maximization in (2) and (3) is over the weights given a chosen architecture. In this work, we consider the case when the inputs x are images, and we want the encoder to also output image-shaped encodings (224×224 RGB images inputs, and three channel 28×28 encoded outputs, in our experiments). Here, we use convolutional layers and spatial pooling layers in both the classifier and encoder architectures. The encoder employs downsampling to produce lower resolution encoded outputs, and its final layer is followed by a *tanh* non-linearity to produce outputs that saturate between $[-1.0, 1.0]$.

Gradient Updates and Minimizing Orbits. Training the encoder proceeds by applying alternating gradient updates to the encoder and classifier, or in the case of (3), classifiers. These gradients are computed on mini-batches of training data for the classification tasks. We find it empirically helpful to use different batches to update the classifiers, and to update the encoder. Note that updating the encoder requires back-propagating gradients through the classifiers.

The classifiers take gradient steps to minimize their losses with respect to the true labels of the encoded data. When optimizing with the desirable attribute classifier, the encoder's update is also based on minimizing that classifier's loss (with a weight of α). However, when computing gradients with respect to the private attribute classifier, we do not use the negative loss—as indicated in (1)—or even the log-loss with respect to the incorrect label, as used in GAN training (Goodfellow et al., 2014a). We find that with both of these approaches, the encoder tries to push the private classifier to predict the incorrect label on a large subset of images with *high confidence*. However, once the encoder has achieved this goal, the classifier is able to quickly recover by simply reversing its labels (true for false, and vice-versa).

This leads to the encoder and classifier making orbits during encoder training, and the classifier being able to easily recover once the encoder is fixed. Therefore, we find a consider a different loss for updating the encoder for the private task: we update it to minimize the loss of the classifier with respect to the *opposite of its current prediction*. Note that the stationary point of this loss is the classifier predicting equal probabilities for true and false for all images, implying that positive and negative examples being indistinguishable. Empirically, this loss proves crucial to learning encoders that have a permanent effect on private classification ability.

Stability with Batch Normalization. As mentioned above, a trivial solution to (1) is for the encoder to output a constant for all images. And indeed, without any further constraints, training moves rapidly to such a degenerate solution. We enforce the zero mean and unit variance constraints on the encoder outputs (in practice, we enforce these on pre-*tanh* outputs) by using batch statistics as a proxy for population statistics, i.e., we simply employ batch-normalization (Ioffe & Szegedy, 2015) after the output of the final layer, without any further learnable weight or bias parameters. Note that traditional batch-normalization for convolutional outputs imposes constraints on mean and variances computed not just across different images in a batch, but also across spatial locations.

However, in our framework these constraints are defined on every element of the encoded output, i.e., we require that the values of a specific channel at a specific pixel location, when averaged across all images, have zero mean and unit variance. And indeed, such a constraint is necessary, because without it, we find that the encoder learns to simply produce the same encoded output for all input images, with variation across spatial locations in the output, but not across different inputs. (It is able to achieve this by detecting borders of the input image). Therefore, we used a modified form of “per-location” batch normalization that treated the output of the final convolutional layer as a single large vector, and computed statistics averaging over the batch, but

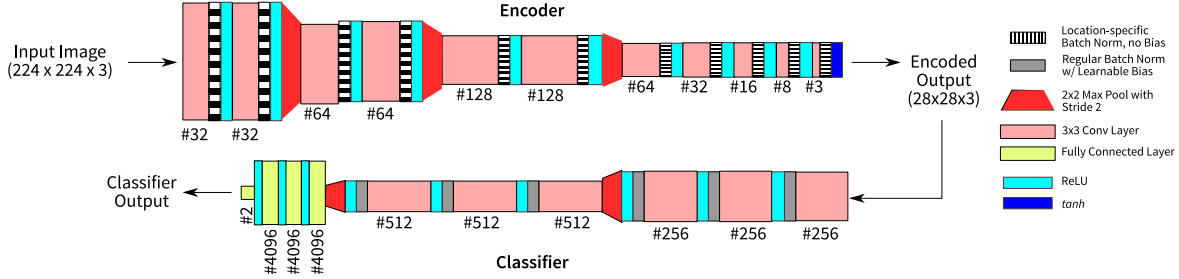


Figure 2. **Encoder and Classifier Architectures.** We use convolutional architectures for both the encoder and classifier networks. Note that for the encoder, we use location specific batch normalization, without biases, after every layer to prevent the encoder from saturating to the trivial solution of producing a constant image.

not over spatial dimensions. However, there still remains a strong gradient signal that often causes intermediate layer activations to saturate—since the loss function continues to direct the encoder towards producing the trivial solution of a constant output.

Even with batch normalization after the final layer, we often found that hidden layer activations would be driven to saturation, causing a constant output at the final layer (at which point, batch-variance of the output would go to zero, and batch normalization would not be effective). Moreover, once all the activations of the hidden layer saturated, the weights of that layer stopped receiving gradients, causing the encoder to remain stuck at that solution. To address this, we included per-location batch normalization *at every layer*, and removed biases all together from the encoder network. This ensured that the outputs of all intermediate layers maintained diversity throughout training, and avoided saturating at a constant output.

As demonstrated next, these strategies allowed our framework to produce useful encoding functions that successfully inhibited inference of chosen private attributes.

4. Experimental Results

Preliminaries. We evaluate our framework on its ability to inhibit identification of specific scene categories, using images from the Places-365 dataset (Zhou et al., 2017). We frame each of these as a binary classification task: i.e., whether an image belongs to a specific category or not. After training and fixing an encoder to inhibit a specific category, we evaluate the ability to train a classifier for that category. We also evaluate the impact of that encoder on the ability to train a classifiers *other* categories.

For each identification task, we train and evaluate classifiers on a balanced dataset where half the images belong to that category—therefore, the “prior” for each task is chance. These sets are constructed from two groups of ten categories

each, from Places-365¹. The negative examples for each category identification task (for training and evaluation), were uniformly sampled from other nine categories in the same group. Therefore, there is overlap between the tasks of identifying categories within the same group (inhibiting identification of a category implies confounding it with other categories in the same group), but not in different groups. Note that we construct non-overlapping training, validation, and testing sets from the official Places-365 training set.

We assumed that the input to our encoder would be RGB images of a fixed resolution of size 224×224 . These were constructed from the Places-365 images—with random scaling and crops for data augmentation during training, and a fixed scale and center-crop for evaluation. The encoder produced three channel 28×28 images as outputs, and these were provided as input to the classification networks. The architectures of both the encoder and classification networks (we used the same architecture for all tasks) are shown in Fig. 3.1. As described in Sec. 3, the encoder used location-specific batch normalization without biases after each layer.

Encoder Training. We learn four encoders, each of which is trained to inhibit identification of a different scene class—arch, army base, airport terminal, and airfield—all from group 1. These encoders are trained based on (1), with only the generic variance constraint. We also train a fifth encoder to inhibit the inference of the “army base” class, but to support inference of the “airport terminal” class, based on (4) with $\alpha = 1/16$. We train these encoders as described in Sec. 3. We use the Adam optimizer (Kingma & Ba, 2014) and train for a total of 860k iterations.

We begin by training the classifier for 5k iterations as “warm up” against a randomly initialized encoder, and then proceed with alternating updates to the encoder and classifiers. The

¹**Group 1:** arch, army base, airport terminal, airfield, alley, arena hockey, amusement park, apartment building, aquarium, arena rodeo. **Group 2:** amphitheater, auto showroom, airplane cabin, archaeological excavation, art studio, artists loft, assembly line, athletic field, atrium, auto factory.

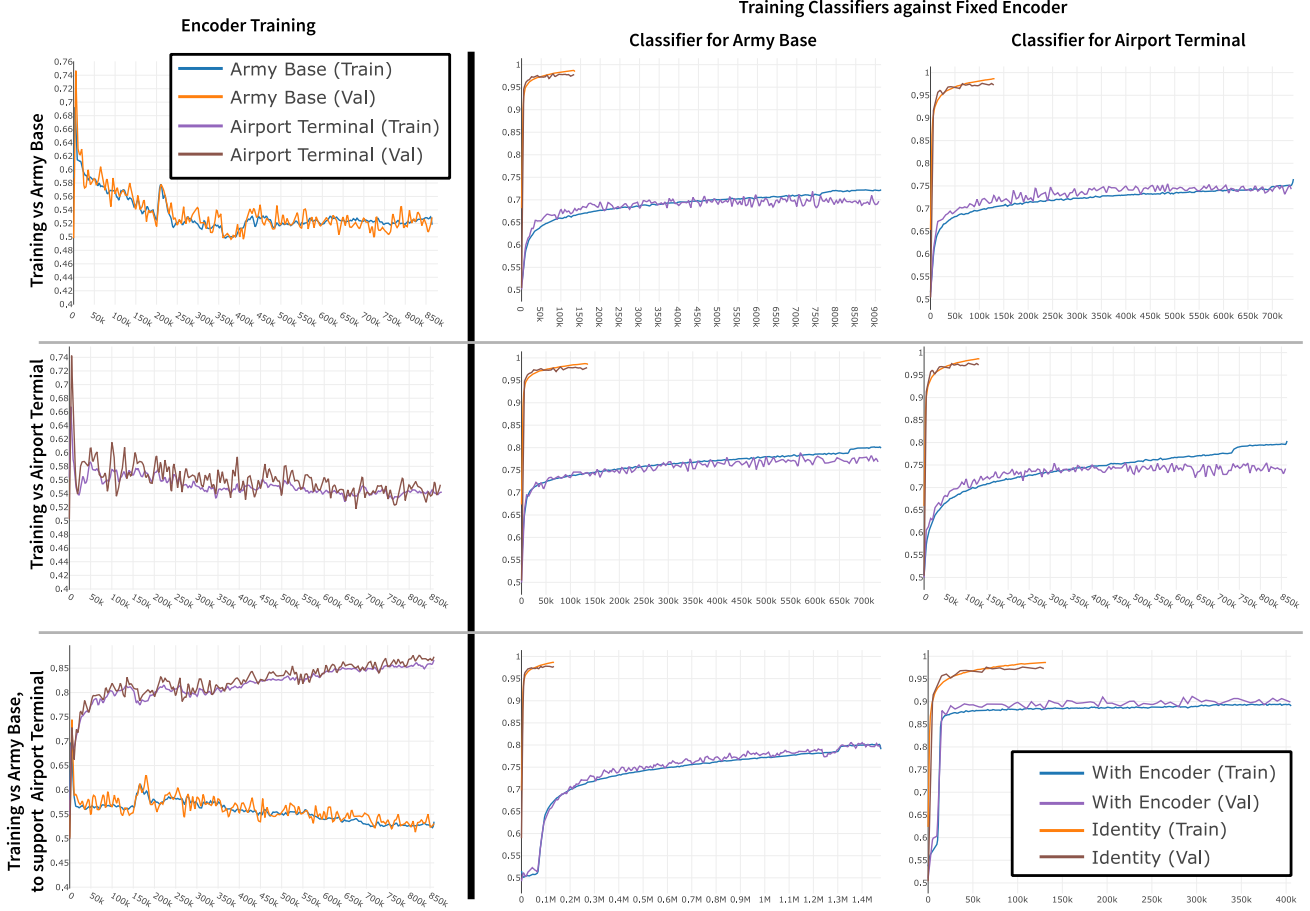


Figure 3. Evolution of Training and Validation Accuracy during and after Encoder Training. We focus here on three encoders. Each row shows the evolution of a different encoder. In the top two rows, the first column shows training and validation accuracy of classifiers training adversarially against an encoder which aims to inhibit army base in the first row and airport terminal in the second. Note that the encoder succeeds at inhibiting both networks from solving their respective tasks. The next two columns show that even after the encoder is fixed, new classifiers trained with access to the encoder training data still fail. Additionally, they show that classifiers trained on the baselines converge much faster and with better performance than those trained on the fixed encoders. In the last row we depict an encoder trained to inhibit army base while promoting airport terminal. In the last row of the first column, we show the encoder training adversarially against a network, which aims to solve the private task (army base) and in collusion with a network, which aims to solve the desired task (airport terminal). Note that the encoder succeeds at inhibiting the private task while allowing the desired task to succeed. In the next two columns of the last row, the encoder is fixed. Here new classifiers trained with access to the fixed encoder still fail. In addition, the next two columns of the last row show that classifiers trained with the baselines learn earlier and to a higher rate than those trained with the fixed encoder.

learning rate for the classifier is kept fixed at 10^{-4} . For the encoder, we begin with a rate of 10^{-4} , but then drop it by a factor of $(0.1)^{1/4}$ every 200k iterations. Empirically, dropping the learning rate has a significant effect on subsequent classification performance after the encoder is fixed, since the encoder now trains to inhibit a classifier that is able to adapt at increasingly faster relative rates.

Figure 3 (left column) illustrates the evolution of classifier accuracy for some of these encoders—including the fifth encoder where we show accuracies for both the private and desirable attributes. We see that the encoder holds the

private classifier accuracy at a low value, even as its learning rate continues to drop—although there are occasional increases in private accuracy around learning rate drops. The learned encoding functions themselves are visualized in Fig. 1, where we show examples of typically encoded images for each encoder. To better show the variability between images, we map the encoder output to an RGB image by mapping the value at each location and channel to a histogram equalized value—i.e., we compute a histogram of values at that location and channel across images, and map a value to its quantile in the histogram.

Encoder	Binary Scene Classification Tasks							
	Arch	Army	Airport Terminal	Airfield	Alley	Arena, Hockey	†Amphitheater	†Auto Showroom
Identity	.942	.983	.967	.982	.969	.995	.951	.958
Naive Blur	.782	.914	.869	.951	.881	.966	.843	.898
Learned								
-Arch	.727	.835	.816	.917	.852	.931	.836	.873
-Army Base	.639	.689	.743	.886	.773	.875	.770	.805
-Airport Terminal	.688	.780	.748	.892	.812	.912	.774	.845
-Airfield	.615	.694	.679	.856	.740	.839	.742	.708
-Army Base +Airport Terminal	.710	.803	.902	.914	.831	.899	.832	.832

† Categories from Group 2.

Table 1. Test Set Scene Identification Accuracies with Different Encoders. The columns depict 8 binary classification tasks that we create from categories taken from the Places-365 dataset. In the first row, we show the test accuracy for a VGG16-like network trained on the original images (identity encoder). In the second row, we show the test accuracy for the classifier network shown in Fig. 1 trained with blurred images. In the **Learned** results, we show the test accuracy for the classifier network shown in Fig. 1 classifier trained on the outputs of four *fixed* encoders trained with our optimization for arch, army-base, airport and air-field as the private tasks. The first four encoders optimize using a generic objective maintaining variance in the encoder output. The red boxes show the inhibited task’s test accuracy beats the baselines. In addition, the generic object preserves information for other tasks in 7 out of 8 categories. The last row shows the test accuracy for the outputs of a *fixed* encoder trained with our generic objective, and optimized to promote a desired task. The red box shows the inhibited task beats the baselines, and the green box shows that the test accuracy for the desired task beats naive blur and is comparable to the identity baseline.

Evaluation. Having trained the encoders, we next evaluate the ability of a classifier to learn to solve each of the label classification tasks from the encoded images. To evaluate this, we train classifiers from scratch, for each task and each encoder. In addition to the learned encoders above, we also train classifiers against a blur baseline—which produces a 28×28 images by applying an 120×120 averaging filter (our encoder’s receptive field is 112×112) and downsampling by a factor of 8—as well as classifiers trained on the original images themselves (these classifiers use larger architectures to handle full-resolution inputs). We train all classifiers also using Adam, with an initial learning rate of 10^{-5} for the learned encoders and blur baseline (we empirically found this to be optimal), and 10^{-4} for classifiers on the original images. We also continue training after dropping the learning rate once by a factor of 0.1 after the validation loss saturates.

The second and third columns of Fig. 3 demonstrate the behavior of classifier trained to detect the “army base” and “airport terminal” classes from the outputs of three of our encoders—those trained against “army base” and “airport terminal”, and the one trained against “army base” but to support “airport terminal”. We show both validation and training losses of these classifiers, and compare them to the losses of the “identity” classifiers (those trained on the original images). We see that in each case, while the learned classifiers for the private tasks perform better than they did within encoder training, they saturate to lower validation accuracy values (even though in some cases, the training

accuracy keeps going up as the network resorts to memorization and overfits). In addition to degrading the achievable accuracy at the private tasks, we also find that the learned encoders extract a higher computational cost from training—which now proceeds significantly more slowly in comparison to on the original images (where the networks reach greater than 90% accuracy in less than 100k iterations).

It is also interesting to compare classifier training for the “airport terminal” task on the two encoders trained to inhibit “army base”. The first encoder with a generic variance constraint also removes information relevant to “airport terminal” and affects its inference. The one trained to explicitly support it as a desirable class, however, leads to much better classification accuracy and faster convergence—albeit with an increase in achievable accuracy on the private task.

Table 1 summarizes the final test set accuracy of classifiers for a number of tasks, trained on each of these encoders and the blur baseline. We include the four tasks for which we trained encoders, and two more tasks each from groups 1 and 2. We also report validation accuracy at different points during training in Table 2. We see that in every case, a learned encoder leads to considerable degradation in the accuracy of its corresponding private task, and more so than the blur baseline (which is not adapted to specific tasks).

It is also apparent that some tasks are easier to solve, and therefore harder to inhibit (e.g., see “airfield”). This is likely because some categories have a larger number of redundant cues that are harder to effectively censor. This is why the

Encoder	Binary Scene Classification Tasks								
	Iteration	Arch	Army	Airport Terminal	Airfield	Alley	Arena, Hockey	Amphi-theater	Auto Showroom
Identity	100k	.928	.978	.972	.981	.957	.994	.955	.956
	Final	.935	.979	.972	.983	.962	.994	.957	.949
Naive Blur	100k	.772	.872	.849	.945	.879	.952	.854	.891
	Final	.715	.896	.855	.952	.884	.973	.854	.888
Learned									
-Arch	100k	.663	.769	.790	.900	.834	.912	.816	.840
	500k	.686	.810	.816	n/a	.849	.931	.817	.860
	Final	.726	.816	.816	.900	.850	.935	.830	.852
-Army Base	100k	.591	.680	.706	.866	.740	.838	.735	.760
	500k	.632	.689	.746	.878	.772	.858	.747	n/a
	Final	.638	.699	.739	.885	.779	.873	.742	.796
-Airport Terminal	100k	.628	.733	.721	.887	.795	.861	.771	.777
	500k	.661	.782	.729	n/a	.832	.910	n/a	.833
	Final	.681	.766	.743	.893	.833	.909	.785	.819
-Airfield	100k	.522	.603	.526	.612	.626	.655	.631	.510
	500k	.596	.648	.633	.821	.721	.796	.697	.659
	Final	.628	.683	.679	.878	.756	.823	.720	.711
-Army Base +Airport Terminal	100k	.512	.635	.898	.870	.714	.793	.796	.745
	500k	.659	.747	n/a	.892	.810	.883	.828	.816
	Final	.722	.792	.899	.918	.839	.900	.829	.817

Table 2. **Validation Accuracy vs Training Iterations.** In this table, we compare the training iterations for the two baselines (first two rows) with the **learned** encoders trained using our optimization (last five rows). In this table “final” represents validation accuracies at convergence. The baselines achieve high validation accuracies within a few iterations, much before 500k iterations. On the other hand, our fixed encoders delay convergence significantly, and at 500k iterations all the networks training on the private tasks are still training and are yet to converge. Each of these networks eventually converge to a final value shown in each red box and that is lower than the baselines. In the last row we show the validation accuracies for the encoder aims not only to inhibit a private task, but also prioritize maintaining information for a desired task. When the network that is training on the private task converges (red box) the positive task (green box) has a validation accuracy comparable to baselines.

learned encoders have different degrees of success in censoring different tasks. Interestingly, censoring “easy” private tasks (like “airfield”) leads to overall poorer performance for other tasks as well, likely due to the encoder being forced to remove a lot of information that may also be useful for other tasks. Meanwhile, the encoder trained against a task that degrades quickly, such as “arch”, is able to automatically preserve more information in its encoded outputs.

These results demonstrate that our method is able to automatically discover and remove information related to sensitive private attributes, permanently inhibiting the inference of these attributes—both in terms of achievable accuracy, and slower training.

5. Conclusion

We presented a framework to automatically learn encoding functions that remove information from high-dimensional

data related to sensitive private tasks. Our framework achieved this by formulating an adversarial optimization problem between the encoding function and estimators for the private tasks. We modeled both the encoder and estimator as neural networks, and described an effective strategy for optimization. Experimental results on tasks of real-world complexity validated the efficacy of our approach.

Note that we did not constrain our encoded outputs to appear natural, or resemble the original data. Consequently, our framework requires classifiers for the desirable tasks to also be retrained. Others (e.g., [Meden et al. \(2018\)](#); [Brkic et al. \(2017\)](#); [Di et al. \(2017\)](#)) have successfully incorporated such requirements in different approaches to privacy and censorship, and one of our goals in future work is to extend our framework in a similar manner.

Acknowledgments. FP and SJK received support for this work from U.S. Department of Homeland Security under Grant Award Number, 2014-DN-077-ARI083. The views and conclusions contained in this document are those of the authors and should not be

interpreted as necessarily representing the official policies, either expressed or implied, of the Department of Homeland Security. AC thanks NVIDIA corporation for the donation of a Titan X GPU used in this research.

References

- Agrawal, P. and Narayanan, P. Person de-identification in videos. *IEEE Transactions on Circuits and Systems for Video Technology*, 2011.
- Arjovsky, Martin and Bottou, Léon. Towards principled methods for training generative adversarial networks. In *NIPS Workshop on Adversarial Training*, 2016.
- Boyle, Michael, Edwards, Christopher, and Greenberg, Saul. The effects of filtered video on awareness and privacy. 2000.
- Brkic, Karla, Sikiric, Ivan, Hrkac, Tomislav, and Kalafatic, Zoran. I know that person: Generative full body and face de-identification of people in images. *CVPRW*, 1(2):4, 2017.
- Chen, D., Chang, Y., Yan, R., and Yang, J. Tools for protecting the privacy of specific individuals in video. *EURASIP Journal on Advanced Signal Processing*, 2006.
- Di, Xing, Sindagi, Vishwanath A, and Patel, Vishal M. Gp-gan: Gender preserving gan for synthesizing faces from landmarks. *arXiv preprint arXiv:1710.00962*, 2017.
- Driessen, B. and Durmuth, M. Achieving anonymity against major face recognition algorithms. *Lecture notes in computer science*, 2013.
- Dwork, Cynthia. Differential privacy: A survey of results. In *International Conference on Theory and Applications of Models of Computation*, pp. 1–19. Springer, 2008.
- Edwards, Harrison and Storkey, Amos. Censoring representations with an adversary. *arXiv preprint arXiv:1511.05897*, 2015.
- Goodfellow, Ian, Pouget-Abadie, Jean, Mirza, Mehdi, Xu, Bing, Warde-Farley, David, Ozair, Sherjil, Courville, Aaron, and Bengio, Yoshua. Generative adversarial nets. In *Advances in neural information processing systems*, pp. 2672–2680, 2014a.
- Goodfellow, Ian J, Shlens, Jonathon, and Szegedy, Christian. Explaining and harnessing adversarial examples. *arXiv preprint arXiv:1412.6572*, 2014b.
- Gross, R., Sweeney, L., de la Torre, F., and Baker, S. Semi-supervised learning of multi-factor models for face de-identification. *CVPR*, 2008.
- Ioffe, Sergey and Szegedy, Christian. Batch normalization: Accelerating deep network training by reducing internal covariate shift. In *Proc. ICML*, 2015.
- Kingma, Diederik P and Ba, Jimmy. Adam: A method for stochastic optimization. *arXiv preprint arXiv:1412.6980*, 2014.
- Meden, Blaž, Emeršič, Žiga, Štruc, Vitomir, and Peer, Peter. k-same-net: k-anonymity with generative deep neural networks for face deidentification. *Entropy*, 20(1):60, 2018.
- Moosavi Dezfooli, Seyed Mohsen, Fawzi, Alhussein, and Frossard, Pascal. Deepfool: a simple and accurate method to fool deep neural networks. In *Proc CVPR*, 2016.
- Moosavi-Dezfooli, Seyed-Mohsen, Fawzi, Alhussein, Fawzi, Omar, and Frossard, Pascal. Universal adversarial perturbations. In *Proc CVPR*, 2017.
- Nguyen, Anh, Yosinski, Jason, and Clune, Jeff. Deep neural networks are easily fooled: High confidence predictions for unrecognizable images. In *Proc. CVPR*, 2015.
- Raval, Nisarg, Machanavajjhala, Ashwin, and Cox, Landon P. Protecting visual secrets using adversarial nets. In *Computer Vision and Pattern Recognition Workshops (CVPRW)*, 2017 *IEEE Conference on*, pp. 1329–1332. IEEE, 2017.
- Sweeney, L. k-anonymity: A model for protecting privacy. *International Journal on Uncertainty, Fuzziness and Knowledge-based Systems*, 2002.
- Vasiljevic, Igor, Chakrabarti, Ayan, and Shakhnarovich, Gregory. Examining the impact of blur on recognition by convolutional networks. *arXiv preprint arXiv:1611.05760*, 2016.
- Yu, X., Chinomi, K., Koshimizu, T., Nitta, N., Ito, Y., and Babaguchi, N. Privacy protecting visual processing for secure video surveillance. *IEEE ICIP*, 2008.
- Zhou, Bolei, Lapedriza, Agata, Khosla, Aditya, Oliva, Aude, and Torralba, Antonio. Places: A 10 million image database for scene recognition. *IEEE Transactions on Pattern Analysis and Machine Intelligence*, 2017.